Nanoparticle Encapsulation of Mitaplatin and the Effect Thereof on *In Vivo* Properties

Timothy C. Johnstone,[†] Nora Kulak,[†] Eric M. Pridgen,[‡] Omid C. Farokhzad,[⊥] Robert Langer,[‡,§] and Stephen J. Lippard[†,*]

[†]Department of Chemistry, [‡]Department of Chemical Engineering, and [§]Koch Institute for Integrative Cancer Research, Massachusetts Institute of Technology, Cambridge, Massachusetts 02139, United States, and [⊥]Department of Anesthesiology, Brigham and Women's Hospital, Harvard Medical School, Boston, Massachusetts 02115, United States

ABSTRACT Nanoparticle (NP) therapeutics have the potential to significantly alter the *in vivo* biological properties of the pharmaceutically active agents that they carry. Here we describe the development of a polymeric NP, termed M-NP, comprising poly(D,L-lactic-*co*-glycolic acid)-*block*-poly(ethylene glycol) (PLGA-PEG), stabilized with poly(vinyl alcohol) (PVA), and loaded with a water-soluble platinum(IV) [Pt(IV)] prodrug, mitaplatin. Mitaplatin, *c,c,t*-$[PtCl_2(NH_3)_2(OOCCHCl_2)_2]$, is a compound designed to release cisplatin, an anticancer drug in widespread clinical use, and the orphan drug dichloroacetate following chemical reduction. An optimized preparation of M-NP by double emulsion and its physical characterization are reported, and the influence of encapsulation on the properties of the platinum agent is evaluated *in vivo*. Encapsulation increases the circulation time of Pt in the bloodstream of rats. The biodistribution of Pt in mice is also affected by nanoparticle encapsulation, resulting in reduced accumulation in the kidneys. Finally, the efficacy of both free mitaplatin and M-NP, measured by tumor growth inhibition in a mouse xenograft model of triple-negative breast cancer, reveals that controlled release of mitaplatin over time from the nanoparticle treatment produces long-term efficacy comparable to that of free mitaplatin, which might limit toxic side effects.

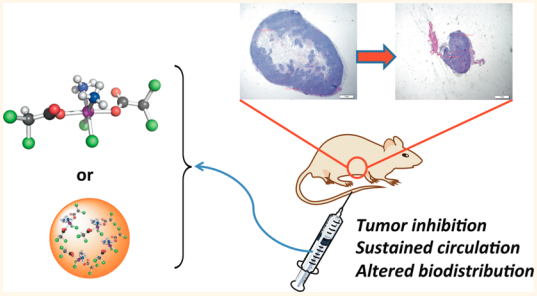

KEYWORDS: mitaplatin · cisplatin · Pt(IV) prodrug · polymer nanoparticle · PLGA-PEG · triple-negative breast cancer

Following its introduction into clinical treatment of cancer in the 1970s, cisplatin has become one of the most widely prescribed anti-tumor drugs.[1] It is commonly used as first-line therapy for blood cancers such as lymphoma and myeloma, as well as many solid tumors including ovarian, bladder, stomach, non-small cell lung, small cell lung, and especially testicular, where it has remarkable efficacy.[2,3] Once cisplatin was added to the chemotherapeutic arsenal, the cure rate for testicular cancer rose to >85%.[4] In breast cancer, however, response rates of only 10% are realized when cisplatin is used as a single agent in pretreated patients.[5] A desire for increased efficacy, the presence of numerous side effects, and the development of tumor recurrence have prompted the scientific community to develop subsequent generations of platinum-based anticancer agents.[6] To date, only two other platinum compounds, carboplatin and oxaliplatin, have been approved by the FDA, and it is of note in the present context that both are Pt(II) complexes.

Despite the emphasis on square-planar Pt(II) compounds as drug candidates, it has been known since the earliest experiments of Rosenberg that Pt(IV) compounds also exhibit anticancer properties.[7] More recently, Pt(IV) compounds have been designed as prodrugs that release active Pt(II) species following chemical reduction in the environment of cancerous cells.[8] The formulation of a platinum anticancer agent as a Pt(IV) construct has several advantages.[9] The greater degree of kinetic inertness of octahedral Pt(IV) centers[10] limits off-target reactivity, and the two additional ligands over square-planar Pt(II) complexes can be used to tune the physical and pharmacokinetic properties of the complex.[11,12]

* Address correspondence to lippard@mit.edu.

Received for review April 17, 2013 and accepted May 17, 2013.

Published online May 22, 2013
10.1021/nn401905g

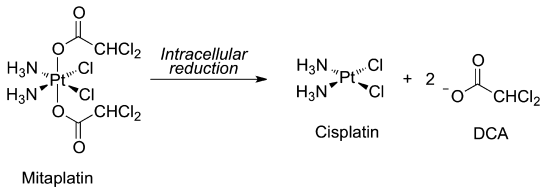

Scheme 1. Proposed mechanism of activation of mitaplatin. Intracellular reduction produces cisplatin and releases two equivalents of DCA.

Another reason for designing Pt(IV) prodrugs is to incorporate bioactive ligands that are released upon reduction. The detached ligands and active Pt(II) moiety then act in concert to provide a dual-threat attack on cancer cells.[13,14] Previously, we reported the preparation of such a Pt(IV) prodrug, mitaplatin (Scheme 1), designed to release two equivalents of dichloroacetate (DCA) and one equivalent of cisplatin upon reduction in the cancer cell.[15] DCA targets the mitochondria and is currently under investigation as a cancer therapeutic that attacks the unique metabolic profile of tumor cells.[16] Mitaplatin capitalizes on the ability of DCA to prime the mitochondria of cancer cells for apoptosis, which is induced by platination of nuclear DNA.[15]

Given that NP therapeutics have the potential to significantly alter the *in vivo* biological properties of the pharmaceutically active agents they carry,[17] our lab has developed constructs to deliver platinum anticancer agents based on a variety of platforms including single-walled carbon nanotubes,[18,19] peptides,[20,21] and polymeric NPs.[22−25] Previous work on polymer-based drug delivery systems involved the preparation of Pt(IV) molecules specifically designed for incorporation into a nanodelivery system. In one strategy, hydrophobic ligands were placed at the axial positions of a cisplatin-releasing Pt(IV) prodrug, allowing it to be encapsulated within the hydrophobic core of PLGA-PEG NPs.[22,24,25] In another strategy, Pt(IV) molecules with pendant carboxylates were prepared for covalent conjugation *via* ester linkages to a hydroxyl-functionalized polymer backbone, and the resulting Pt(IV)−polymer conjugate was blended with PLGA-PEG during formulation to develop Pt(IV)-loaded NPs.[23]

On the basis of encouraging results previously described, which demonstrate the beneficial effects of Pt-loaded NP therapeutics,[24,25] we investigated mitaplatin encapsulated in a PLGA-PEG NP. Because the chemical composition of the axial ligands of this molecule is critical, they cannot be altered to render this hydrophilic molecule amenable to encapsulation *via* either the nanoprecipitation[22,24,25] or conjugation methods[15,19,20,23] previously employed. Instead, an alternative encapsulation strategy, based on a water/oil/water double emulsion,[26] was used. Here we present the preparation and characterization of a PLGA-PEG NP drug delivery construct loaded with mitaplatin, M-NP. We compare M-NP with unencapsulated mitaplatin,

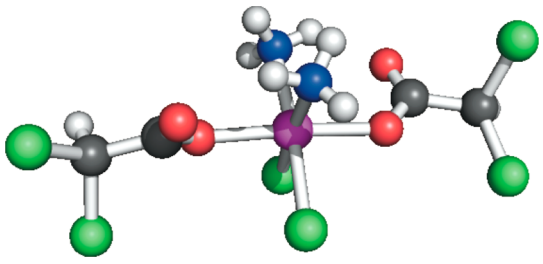

Figure 1. Ball and stick representation of mitaplatin from the crystal structure of mitaplatin·2DMSO. Chlorine atoms are shown in green, oxygen in red, carbon in dark gray, nitrogen in blue, hydrogen in white, and platinum in magenta.

specifically, measuring plasma half-life in rats (pharmacokinetics, PK), ability to inhibit tumor growth in a mouse xenograft model of triple-negative breast cancer (efficacy), and accumulation in the liver and kidneys of mice (biodistribution, BD). This particular cancer was modeled because of the prospect that platinum-based chemotherapy may be effective against this otherwise intractable class of tumors.[27,28]

RESULTS AND DISCUSSION

Synthesis and Characterization. The mitaplatin used in this study was prepared in a manner analogous to that reported earlier.[15] Briefly, *c,c,t*-[$PtCl_2(NH_3)_2(OH)_2$] was suspended in a DMF solution of dichloroacetic anhydride and heated until all of the material dissolved. The final product precipitated upon addition of diethyl ether, but difficulties were encountered during isolation of the product from the DMF reaction mixture. We therefore devised an alternative synthesis of the compound using neat dichloroacetic anhydride as the solvent. This reaction follows a strategy used in the synthesis of other Pt(IV) carboxylate complexes.[29] The reaction time is longer, but no effort was made to optimize the conditions. The yield (80%) was higher than that obtained using DMF as solvent (55%). The product obtained displayed spectroscopic features consistent with its proposed structure. Further discussion of the ^{1}H NMR spectrum is presented in the Supporting Information.

Crystallography. The crystal structures of DMF and DMSO solvates of mitaplatin were solved, and a molecular representation of the platinum complex from the latter is shown in Figure 1. Details of the solution and refinement of the crystal structures are presented in Supporting Information.

Nanoencapsulation. Attempts to encapsulate mitaplatin by standard solvent evaporation nanoprecipitation methods were unsuccessful (data not shown), and we ascribe this failure to the high water solubility of the compound. The problem was solved by encapsulation of mitaplatin with the use of a modified solvent evaporation method based on double emulsion.[30] The process is illustrated diagrammatically in Scheme 2. Briefly, in this method, an amphiphilic block copolymer is dissolved in a water-immiscible organic solvent. This

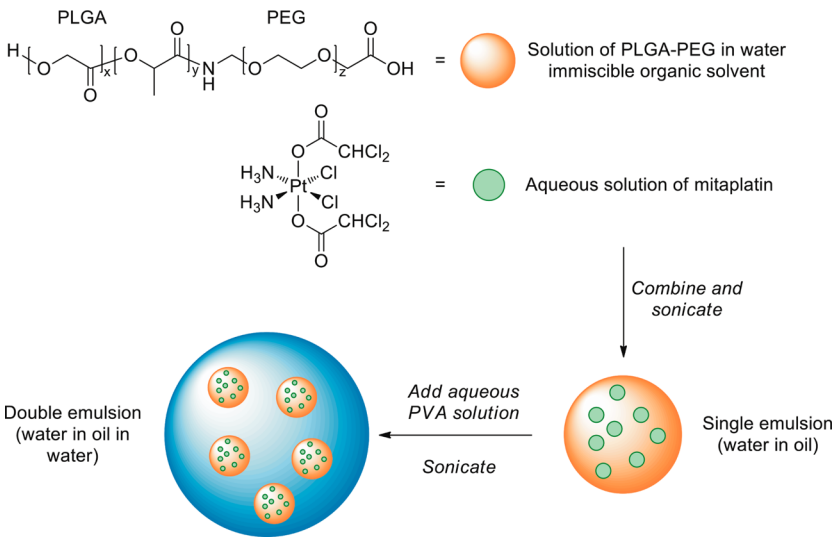

Scheme 2. Diagrammatic representation of the double emulsion method for encapsulating mitaplatin in PLGA-PEG nanoparticles. PVA = poly(vinyl alcohol).

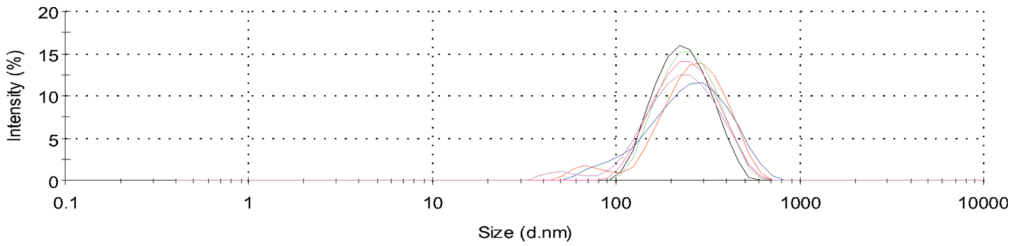

Figure 2. Dynamic light scattering intensity distribution results of multiple replicates of M-NP prepared using optimized conditions (see text).

solution is added to an aqueous solution of the compound to be encapsulated, and the biphasic mixture is sonicated to give a primary "water in oil" emulsion. This emulsified mixture is added to a volume of water containing a surfactant and sonicated again to give a "water in oil in water" double emulsion. Following evaporation of the volatile organic solvent, a suspension of NPs encapsulating the water-soluble molecule is obtained. To our knowledge, this report describes the first example of the use of double emulsion techniques to encapsulate a platinum compound.

The encapsulation was optimized to maximize platinum loading and minimize NP size by varying such parameters as the concentration of the initial polymer solution, the concentration of the initial mitaplatin solution, the ratio of organic solvent to water in the primary emulsion, and the organic solvent used. Any given combination of these was evaluated for platinum loading (% w/w of mitaplatin with respect to polymer in the suspension), NP size, and distribution of sizes as represented by the polydispersity index (PDI). The polymer concentration was 1, 5, or 10 mg/mL, and the mitaplatin concentration was between 1 and 5 mg/mL. The ratio of aqueous to organic solvent in the primary emulsion was 1:10, 1:8, or 1:6, and the organic solvent used was chloroform or a 1:1 mixture of acetone/dichloromethane. Conditions that maximized platinum loading while minimizing size were 5 mg/mL polymer in 1:1 dichloromethane/acetone, 5 mg/mL mitaplatin in water, and a 1:4 aqueous/organic ratio in the primary emulsion. The results for each round of optimization are presented in Table S3. The particles typically displayed a loading of 0.2%, an average size of 208(10) nm, and a PDI of 0.20(2). Representative dynamic light scattering intensity distributions of six batches of nanoparticles obtained by this procedure are presented in Figure 2.

The resulting particles are of adequate size to exploit the enhanced permeability and retention (EPR) effect, a passive targeting mechanism that results from leaky vasculature and poor lymphatic drainage characteristic of rapidly growing tumor tissue.[31]

Controlled Release of Mitaplatin. In order to study the release properties of mitaplatin from the NPs, aliquots of M-NP suspension were dialyzed against phosphate buffered saline (PBS) at 37 °C. The release of platinum, measured by atomic absorption spectroscopy (AAS) in this and subsequent experiments, during dialysis is presented in Figure 3 as the fraction of encapsulated platinum released over time. A substantial burst phase is present, and approximately 90% of the platinum is released within the first day.

Retention in the Bloodstream. An important aspect of a pharmacologically active compound that is administered intravenously is its residence time in the bloodstream. A rat model was used to evaluate bloodstream retention of mitaplatin when the compound was administered as either a free agent or a NP formulation. Free mitaplatin is quickly cleared from the blood; 30 min following injection of free mitaplatin, only 17% of the platinum originally injected remains in circulation (Figure 4). On the other hand, when encapsulated within a polymer nanoparticle, the duration of platinum circulation is prolonged. For instance, 30 min post-injection, 66% of the platinum originally present in the plasma remains when M-NP is administered. The area under the curve of the NP construct is twice that of the free complex. When the earlier *in vitro* release data (Figure 3) were converted to retention values and plotted together with platinum retention in the plasma of rats treated with M-NP, the curves overlay (Figure 4). This correlation provides confirmation that the *in vitro* release study accurately modeled the behavior of our construct *in vivo*. Moreover, it supports the conclusion that the enhanced retention of platinum in the bloodstream is a direct result of the controlled release of mitaplatin from the nanoparticle construct.

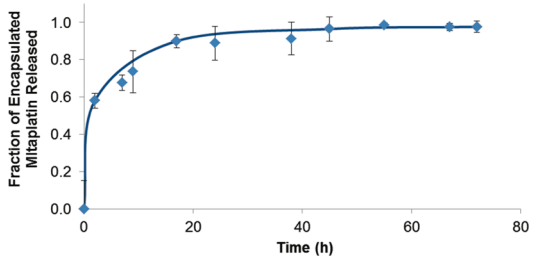

Figure 3. Diffusive release of platinum from M-NP. Error bars represent one standard deviation of the three replicate measurements.

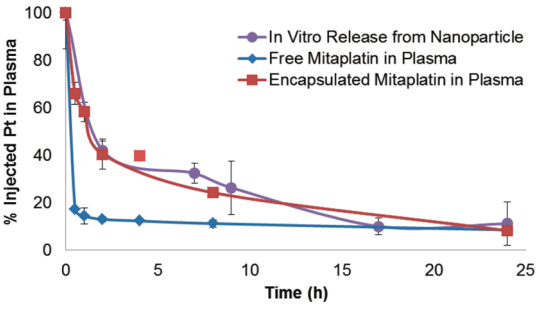

Figure 4. Retention of platinum in the plasma of Sprague–Dawley rats following injection with either free or encapsulated mitaplatin (0.2 mg/kg). Overlaid on these *in vivo* data are the *in vitro* release data. Each point is the average of measurements from three different rats, and error bars represent one standard deviation.

Tumor Growth Inhibition. MDA-MB-468 triple-negative breast cancer cells were used in this study to address the need for therapies to target this class of highly refractory solid tumors.[32] Subcutaneous xenograft tumors were grown in nude mice that were subsequently treated with 1 mg/kg of either unencapsulated mitaplatin or M-NP, both reconstituted in saline. The dosages were computed based on the mass of mitaplatin, and therefore, animals treated with free mitaplatin or M-NP received equal amounts of the active agent. A third cohort of tumor-bearing mice was treated with saline to serve as a negative control. Mice were treated twice a week for two weeks (injections on days 1, 4, 8, and 11) and then monitored for an additional two weeks to observe tumor regrowth. The volume of the tumors during treatment is shown in Figure 5A, and the final tumor volume at the end of the regrowth period is depicted in Figure 5B. At the end of the two week treatment, tumors from mice in the control group had grown significantly, those from the M-NP treated group showed no significant growth as compared to the first day of treatment, and those treated with free mitaplatin showed a reduction in tumor volume. Despite the difference in the short-term effects of free mitaplatin and M-NP, by the end of the regrowth period, both treatments displayed the same degree of tumor growth inhibition. These data are consistent with the theory that the NP serves as a controlled-release delivery vehicle. The same total dose of active platinum agent is being delivered in the two cases, but the concentration of *available* platinum is initially lower in the nanoparticle-treated mice. There is, therefore,

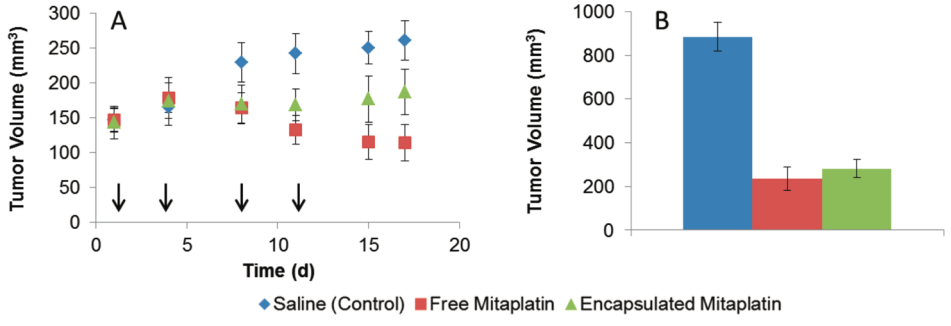

Figure 5. Average size of MDA-MB-468 tumors in a mouse xenograft model (A) during treatment with equal doses (1 mg/kg) of either free or encapsulated mitaplatin and (B) at the end of the tumor regrowth period (day 24). Arrows indicate treatment days. Error bars represent one standard deviation.

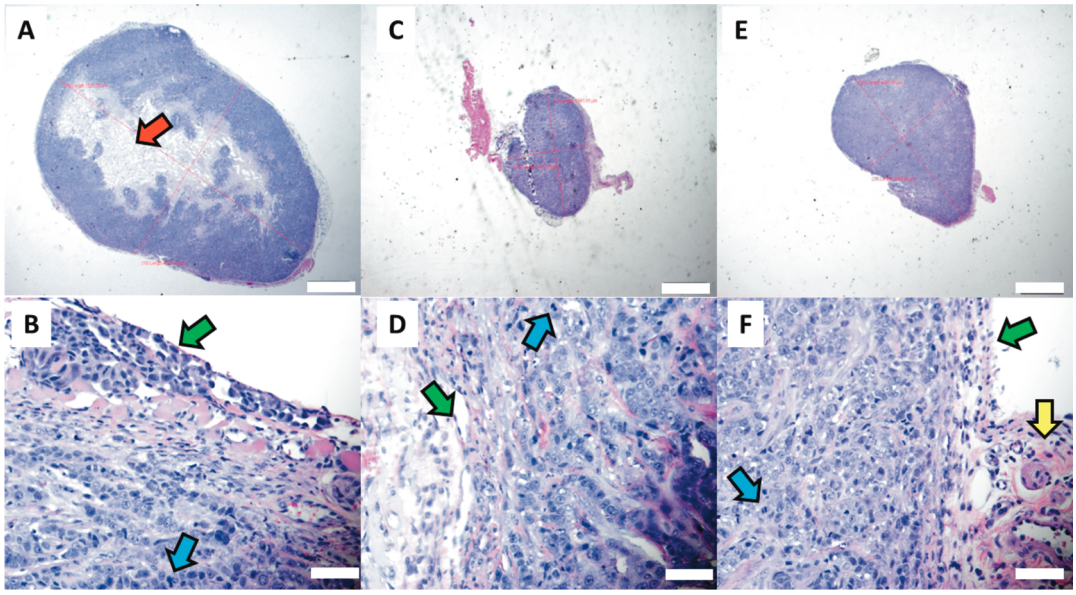

Figure 6. Representative histological images from tumors of mice treated with saline (A and B), free mitaplatin (C and D), or M-NP (E and F). Scale bars in panels A, C, and E are 1 mm and those in panels B, D, and F are 50 μm. The red arrow indicates necrosis. The green arrows indicate vascular/capsular invasion in B and a lack thereof in D and F. The blue arrows highlight isolated instances of mitotic cell division. The yellow arrow indicates a blood vessel from adjacent tissue and the lack of invasion of tumor cells into this vessel is noted.

a greater acute effect observed in the mice treated with free mitaplatin. A controlled release of active agent over time allows the nanoparticle treatment to produce a long-term effect comparable to injection with free mitaplatin. The delayed release may engender less toxicity and improve the therapeutic response.

Histopathology. Following sacrifice of the xenograft-bearing animals, tumor tissue was harvested and subjected to histopathological analysis. Representative tumor slices are shown at both low and high magnification in Figure 6. The low-magnification images highlight the difference between the sizes of the tumors in mice treated with either saline or one of the two mitaplatin formulations, as also depicted in Figure 5. Moreover, there is significantly more necrotic tissue at the center of the control tumor (Figure 6A), consistent with rapid uncontrolled growth. In the high-magnification images, the aggressive invasion of the cancer cells into surrounding tissue can be seen in the control tumors (Figure 6B, green arrow) but is absent in the tumors of the mice treated with either free mitaplatin or M-NP (Figure 6D,F, green arrows). In the latter two cases, the tumors are well capsulated. One section from a tumor of each animal was analyzed and scored according to the overall prevalence of features indicative of aggressive tumor growth including prominent nucleoli, vascular and capsular invasion, mitosis, and necrosis. Isolated instances of these features can be observed in Figure 6B,D,F (highlighted with arrows). The results were averaged across the animals from each group (detailed results presented in Table S4) and indicated that the tumors from the control group were the most robust and aggressive, those from the mitaplatin-treated group were the least aggressive, and those from the M-NP-treated group were intermediate.

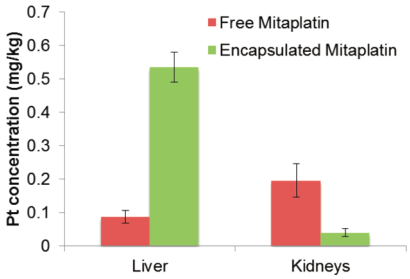

Figure 7. Concentration of platinum in liver and kidney tissues of the mice treated with either free mitaplatin or nanoparticle-encapsulated mitaplatin (1 mg/kg). Error bars represent one standard deviation.

Biodistribution. Although the long-term anti-tumor outcome of the two treatments is similar, drastic differences are present in the biodistribution of platinum in tumor-bearing mice. Treatment with free mitaplatin results in a significant accumulation of platinum in the kidneys (Figure 7). This accumulation is expected because the active complex derived from the reduction of the mitaplatin prodrug is cisplatin, which is dose-limited by nephrotoxicity in the absence of aggressive prehydration.[33] Encapsulation of mitaplatin within the polymer nanoparticle shifts the biodistribution of platinum from the kidneys to the liver. This shift is not surprising because the reticuloendothelial system (RES) would filter the nanoparticles from the bloodstream and the platinum is trapped within the nanoparticles. In addition to the blood retention study and its correlation with the *in vitro* controlled-release

study, this hepatic platinum accumulation provides further evidence in support of the ability of the nanoparticles to carry the platinum complex through the bloodstream. In mice treated with M-NP, the concentration of platinum in the kidneys is less than that in the kidneys of the animals treated with free mitaplatin. Given that nephrotoxicity is a common side effect of platinum treatment,[34] whereas hepatotoxicity is less commonly encountered,[35] we expect that the benefit of the decrease in kidney uptake may be greater than the possible harm incurred by increased accumulation in the liver. Clearly it would be advantageous to avoid clearance by the RES and increase blood circulation time even further. It is possible that this goal could be achieved by reducing the size of the nanoparticles below 100 nm.[36]

Nanoparticle Protection of Mitaplatin. Complexes containing Pt(II) ions are typically kinetically labile, and one impetus for investigating Pt(IV) prodrugs is their comparatively greater kinetic inertness.[9] This reduced reactivity is expected to translate into sustained circulation *in vivo* during which the masked Pt(II) pharmacophore remains safe from deactivation by biological nucleophiles. Only upon entering the reducing environment of the cancer cell is the complex supposed to be reduced, releasing the active Pt(II) agent.[37] A growing body of work shows, however, that certain Pt(IV) prodrugs reduce prematurely in the bloodstream prior to cellular uptake.[8,38−42] Moreover, recent work on the aquation of Pt(IV) prodrugs bearing axial halogenated carboxylate ligands has called their supposed chemical inertness into question.[43] We propose that nanoparticle encapsulation provides the guest platinum complex an additional degree of protection from reductants and nucleophiles by physically preventing interaction between these agents and the encapsulated platinum complex.

The results described in this report provide evidence to support the theory that the nanoparticle protects the encapsulated mitaplatin. Unprotected mitaplatin is rapidly cleared from the bloodstream, whereas the construct containing encapsulated mitaplatin displays prolonged circulation. The *in vitro* release study corroborates the hypothesis that this retention of platinum in the bloodstream is the result of controlled release from the nanoparticle. Moreover, following treatment with M-NP, platinum does not accumulate in the kidneys as it does in mice treated with free mitaplatin. Instead, platinum accumulates in the organs of the reticuloendothelial system, which is responsible for removing colloidal objects, such as polymer nanoparticles, from the bloodstream. Although these data are consistent with the scheme in which the platinum complex is protected within the nanoparticle, the AAS measurements do not provide direct information about the oxidation state or chemical identity of the platinum that is associated with the nanoparticle. Experiments are underway in our lab to directly investigate the effect of encapsulation on the rate of reduction of encapsulated Pt(IV) prodrugs in blood and cells.

CONCLUSIONS

We demonstrate here that a hydrophilic platinum anticancer agent, mitaplatin, can be encapsulated within PLGA-PEG NPs. Encapsulation within these NPs prolongs retention of platinum in the bloodstream over that observed when unencapsulated mitaplatin is administered. This increased retention correlates well with *in vitro* release studies and is corroborated by redirection of platinum to the liver. Both unencapsulated mitaplatin and M-NP reduced the tumor burden of mice carrying MDA-MB-468 triple-negative breast cancer xenografts. The unencapsulated mitaplatin displayed a greater acute effect but the long-term tumor growth inhibition realized by both treatments was the same. The nanodelivery of the platinum agent significantly shifted the biodistribution of platinum in treated animals away from accumulation in the kidneys, a traditional site of platinum-induced toxicity. This study demonstrates that NP encapsulation can indeed have a favorable influence on the biological activity of a Pt(IV) prodrug. Following optimization of the encapsulation process to further increase Pt loading and minimize particle size, thereby bypassing accumulation in the liver, such a NP treatment could become an attractive candidate for further investigation as a chemotherapeutic treatment for triple-negative breast cancer. Experiments are in progress to use this double emulsion strategy to encapsulate other hydrophilic platinum compounds.

MATERIALS AND METHODS

Materials and Instrumentation. Mitaplatin[15] (*c,c,t*-[$PtCl_2(NH_3)_2$-$(OOCCHCl_2)_2$]) and poly(D,L-lactic-*co*-glycolic acid)-*block*-poly(ethylene glycol)[44] (PLGA-PEG) were synthesized as previously reported. Poly(vinyl alcohol) (PVA, MW 30 kDa) was purchased from Sigma-Aldrich. Platinum concentrations were measured by graphite furnace atomic absorption spectroscopy (GFAAS) using a Perkin-Elmer AAnalyst 600 spectrometer outfitted with a transverse heated graphite atomizer. Platinum absorption was measured at 265.9 nm, and a Zeeman background absorption correction was applied.[45,46] Nanoparticle sizes were determined by dynamic light scattering on a Zetasizer Nano (Malvern Instruments). ^{1}H NMR spectroscopic measurements were performed on a Varian Inova-500 spectrometer in the MIT Department of Chemistry Instrumentation Facility with deuterated DMSO as a solvent. NMR chemical shifts (δ) are reported in parts per million with respect to tetramethylsilane and are referenced to residual solvent peaks in the spectrum.

Alternative Mitaplatin Synthesis. A suspension of *c,c,t*-[$PtCl_2$-$(NH_3)_2(OH)_2$][47] (100 mg, 0.3 mmol) in neat dichloroacetic anhydride (3 mL) was stirred at 70 °C for 5 h. The mixture remained a suspension throughout the reaction. Diethyl ether (5 mL) was

added, and the precipitate was collected by vacuum filtration. The solid was washed with diethyl ether and dried under vacuum. Yield: 131 mg of pale yellow solid, 80%. Characterization was identical to that previously reported[15] with an exception as discussed in the Supporting Information.

X-ray Crystallography. Details of the data collection, structure solution, and refinement are provided in Supporting Information.

Nanoprecipitation. Mitaplatin was encapsulated by a modified solvent evaporation method using double emulsion.[30] Parameters were varied as detailed in the Results and Discussion section, but generally, the PLGA-PEG copolymer was dissolved in a water-immiscible organic solvent and mitaplatin was dissolved in Milli-Q water. An aliquot of the polymer solution was combined with an aliquot of the mitaplatin solution, and the mixture was sonicated (10 W, 30 s). The volumes of these aliquots were varied as described in Table S3. This emulsion was then combined with 0.5% aqueous PVA (6.7 mL) and sonicated (10 W, 30 s). This double emulsion was poured into 0.05% aqueous PVA (27 mL) and stirred overnight to allow the volatile organic solvent to evaporate. The resulting mixture, with the characteristic milky blue appearance indicative of a colloidal suspension, was filtered through a 0.2 μm cellulose acetate syringe filter to remove any aggregation products. The filtrate was concentrated using Amicon ultracentrifugation filtration devices (Millipore) with a molecular weight cut-off (MWCO) of 100 kDa. The concentrated suspension of nanoparticles containing mitaplatin (M-NP) was washed twice with Milli-Q water and diluted to a final volume of 500 μL. The platinum content of the suspension was then quantified using GFAAS. Dilutions to concentrations within the linear dynamic range of the spectrometer (50−200 μg Pt/L) were performed with 1:1 water/acetonitrile, a mixture that aided in dissolving the polymer.

Controlled Release of Mitaplatin. A suspension of M-NP was prepared as described above. The suspension was aliquotted (150 μL) into dialysis cassettes outfitted with 3500 Da MWCO membranes. The cassettes were submerged in 12 L of phosphate buffered saline (PBS, pH 7.4) and stirred in the dark at 37 °C. At defined time points (0, 2, 7, 9, 17, 24, 38, 45, 55, 67, and 72 h), three cassettes were removed and the concentration of platinum in each cassette was determined by GFAAS. Reported values are the average of three replicates.

Preparation of Nanoparticles for Animal Studies. Using optimum parameters defined in the Results and Discussion section, large-scale batches of M-NP were prepared for use in animal studies. The preparation was scaled-up by simply performing multiple parallel runs of the double emulsion precipitation as described above and combining the final suspensions. Nanoparticles were always freshly prepared and used within 24 h. The suspensions were kept at 4 °C and transported on ice to prevent premature release of mitaplatin. The final reconstitution/dilution to the concentration needed for any particular animal experiment was performed with PBS (pH 7.4), and the suspension was filtered through 0.2 μm filters to render it sterile.

Animal Studies. Animal experimentation was carried out at Toxikon (Bedford, MA) in full compliance with their Institutional Animal Care and Use Committee (IACUC) regulations, the Association for Assessment and Accreditation of Laboratory Animal Care (AAALAC) International and U.S. federal law.

Platinum Concentrations in Biological Samples. For analysis of plasma samples, 200 μL volumes of plasma were lyophilized. The dry residue was suspended in 400 μL of concentrated HNO_3, boiled for 1 h, and then diluted with 600 μL of 0.1 M HCl.[48] This acidic solution was then analyzed by GFAAS, diluting with water if necessary. The initial concentration of platinum in the plasma was obtained by dividing the amount of platinum that was injected into each rat by the volume of plasma in the rat (4.1 ± 0.3 mL plasma per 100 g body mass).[49]

To determine the concentration of platinum in tissue samples, the samples were first dissolved.[48] To account for possible compartmentalization within the tissue, the entire organ was dissolved rather than digesting only a portion. The tissues were digested with concentrated nitric acid (500 μL/200 mg of tissue) overnight at room temperature. The mixture was then boiled for 3−5 min. Aqueous hydrogen peroxide (30%) was added in a volume equal to the initial amount of acid used. The mixture was stirred for 5 min and then boiled for an additional 3−5 min. The resultant pale yellow solutions were cooled to room temperature and analyzed by GFAAS. The spectroscopy was conducted using parameters adjusted so as to optimize the recovery of platinum from tissue samples.[48]

Retention in the Bloodstream. The subjects of the study were three male Sprague−Dawley rats that weighed approximately 330 g each and were at least 5 weeks old (adult). A sterile solution of mitaplatin or a suspension of M-NP was prepared and diluted with PBS (pH 7.4) to provide a dose of 0.2 mg of mitaplatin/kg of body mass in a volume of 8 mL/kg of body mass. The dose was injected into the lateral tail vein as a single bolus. Blood samples (1 mL) were collected from the lateral tail vein at 0, 0.5, 1, 2, 4, 8, and 24 h post-dose. Each blood sample was portioned in two, and plasma was isolated from one portion by centrifugation at 3000 *g* for 10 min at 4 °C.

Tumor Growth Inhibition. MDA-MB-468 triple-negative breast cancer cells were obtained from American Type Culture Collection (ATCC) and grown in L-15 medium (Invitrogen), 10% fetal bovine serum (FBS), 1% penicillin/streptomycin in T-175 flasks. A suspension of 132 million cells was obtained with 86% viability, pelleted, and resuspended in L-15 medium with 50% Matrigel (BD Biosciences). A 0.25 mL volume of this cell suspension, containing 5×10^6 cells, was injected into the mammary fat pad of adult female BALB/c nude mice with body weights of approximately 15 g each. Tumor nodules were allowed to grow to a volume of 150 mm^3 before treatment began. Tumor length and width were measured with calipers, and the tumor volume was calculated using the formula $V = a \times b^2$ in which a is the length and b is the width. The animals, six per group, were treated (i.v. injection into tail vein) twice a week for two weeks (days 1, 4, 8, and 11) with saline, mitaplatin in PBS (1 mg/kg), or M-NP in PBS (1 mg mitaplatin/kg). After the final dose (day 11), the animals were observed for two more weeks to monitor regrowth of the tumors. During treatment, one animal from the group treated with mitaplatin was sacrificed early due to the development of necrosis in the tail, and the data from this animal were removed from all analyses.

Biodistribution. Following the completion of the tumor growth inhibition study, the mice that were treated with mitaplatin or M-NP were sacrificed and liver and kidney tissue was harvested and digested as described above for analysis by GFAAS.

Histopathology. Additionally, following sacrifice of the animals, tumors were harvested and fixed in 10% neutral-buffered formalin. Thin slices (~5 μm) were prepared and stained with hematoxylin and eosin for histological analysis. This analysis was carried out by Toxikon (Bedford, MA) pathologist Dr. Alex Richter, DVM, MS, DACVP, and Dr. Ying Ping Yu, MD.

Conflict of Interest: The authors declare the following competing financial interest(s): O.C.F., R.L., and S.J.L. declare a financial interest in Blend Therapeutics.

Supporting Information Available: NMR and crystallographic characterization of mitaplatin, detailed outcomes of nanoparticle optimization runs, and tabulation of the histological analysis. Crystallographic material is present in CIF format and has been deposited with the CSD. This material is available free of charge *via* the Internet at http://pubs.acs.org.

Acknowledgment. Dr. S. Dhar is thanked for her assistance in culturing the MDA-MB-468 cells. Dr. G. Y. Park is acknowledged for providing initial samples of mitaplatin used during optimization of the encapsulation. Drs. A. Richter and Y. P. Yu are thanked for their examination of the histological samples and for generous and helpful discussions. This work was supported by NIH Grants 5-U54-CA119349 (R.L.), 5-U54-CA151884 (R.L.), and 5-R01-CA034992 (S.J.L.). E.M.P. is supported by a Center of Cancer Nanotechnology Excellence (CCNE) graduate research fellowship NIH Grant 5-U54-CA151884-02. T.C.J. has received partial funding from the Harvard/MIT CCNE, NIH Grant 5-U54-CA151884. N.K. received a research fellowship from DAAD. Spectroscopic instrumentation at the MIT DCIF is maintained with funding from NIH Grant 1-S10-RR13886-01.

REFERENCES AND NOTES

1. Kelland, L. R.; Farrell, N. *Platinum-Based Drugs in Cancer Therapy*; Humana Press: Totowa, N.J., 2000.
2. Wheate, N. J.; Walker, S.; Craig, G. E.; Oun, R. The Status of Platinum Anticancer Drugs in the Clinic and in Clinical Trials. *Dalton Trans.* **2010**, *39*, 8113–8127.
3. Dank, M.; Zaluski, J.; Barone, C.; Valvere, V.; Yalcin, S.; Peschel, C.; Wenczl, M.; Goker, E.; Cisar, L.; Wang, K.; *et al.* Randomized Phase III Study Comparing Irinotecan Combined with 5-Fluorouracil and Folinic Acid to Cisplatin Combined with 5-Fluorouracil in Chemotherapy Naive Patients with Advanced Adenocarcinoma of the Stomach or Esophagogastric Junction. *Ann. Oncol.* **2008**, *19*, 1450–1457.
4. Einhorn, L. H. Treatment of Testicular Cancer: A New and Improved Model. *J. Clin. Oncol.* **1990**, *8*, 1777–1781.
5. Ott, I.; Gust, R. Preclinical and Clinical Studies on the Use of Platinum Complexes for Breast Cancer Treatment. *Anti-Cancer Agents Med. Chem.* **2007**, *7*, 95–110.
6. Kelland, L. The Resurgence of Platinum-Based Cancer Chemotherapy. *Nat. Rev. Cancer* **2007**, *7*, 573–584.
7. Rosenberg, B.; VanCamp, L.; Trosko, J. E.; Mansour, V. H. Platinum Compounds: A New Class of Potent Antitumour Agents. *Nature* **1969**, *222*, 385–386.
8. Pendyala, L.; Cowens, J. W.; Chheda, G. B.; Dutta, S. P.; Creaven, P. J. Identification of *cis*-Dichloro-bis-isopropylamine Platinum(II) as a Major Metabolite of Iproplatin in Humans. *Cancer Res.* **1988**, *48*, 3533–3536.
9. Hall, M. D.; Mellor, H. R.; Callaghan, R.; Hambley, T. W. Basis for Design and Development of Platinum(IV) Anticancer Complexes. *J. Med. Chem.* **2007**, *50*, 3403–3411.
10. Taube, H. Rates and Mechanisms of Substitution in Inorganic Complexes in Solution. *Chem. Rev.* **1952**, *50*, 69–126.
11. Hambley, T. W.; Battle, A. R.; Deacon, G. B.; Lawrenz, E. T.; Fallon, G. D.; Gatehouse, B. M.; Webster, L. K.; Rainone, S. Modifying the Properties of Platinum(IV) Complexes in Order To Increase Biological Effectiveness. *J. Inorg. Biochem.* **1999**, *77*, 3–12.
12. Gramatica, P.; Papa, E.; Luini, M.; Monti, E.; Gariboldi, M. B.; Ravera, M.; Gabano, E.; Gaviglio, L.; Osella, D. Antiproliferative Pt(IV) Complexes: Synthesis, Biological Activity, and Quantitative Structure−Activity Relationship Modeling. *J. Biol. Inorg. Chem.* **2010**, *15*, 1157–1169.
13. Barnes, K. R.; Kutikov, A.; Lippard, S. J. Synthesis, Characterization, and Cytotoxicity of a Series of Estrogen-Tethered Platinum(IV) Complexes. *Chem. Biol.* **2004**, *11*, 557–564.
14. Ang, W. H.; Khalaila, I.; Allardyce, C. S.; Juillerat-Jeanneret, L.; Dyson, P. J. Rational Design of Platinum(IV) Compounds To Overcome Glutathione-S-Transferase Mediated Drug Resistance. *J. Am. Chem. Soc.* **2005**, *127*, 1382–1383.
15. Dhar, S.; Lippard, S. J. Mitaplatin, a Potent Fusion of Cisplatin and the Orphan Drug Dichloroacetate. *Proc. Natl. Acad. Sci. U.S.A.* **2009**, *106*, 22199–22204.
16. Bonnet, S.; Archer, S. L.; Allalunis-Turner, J.; Haromy, A.; Beaulieu, C.; Thompson, R.; Lee, C. T.; Lopaschuk, G. D.; Puttagunta, L.; Harry, G.; *et al.* A Mitochondria-K^+ Channel Axis Is Suppressed in Cancer and Its Normalization Promotes Apoptosis and Inhibits Cancer Growth. *Cancer Cell* **2007**, *11*, 37–51.
17. Kamaly, N.; Xiao, Z.; Valencia, P. M.; Radovic-Moreno, A. F.; Farokhzad, O. C. Targeted Polymeric Therapeutic Nanoparticles: Design, Development and Clinical Translation. *Chem. Soc. Rev.* **2012**, *41*, 2971–3010.
18. Feazell, R. P.; Nakayama-Ratchford, N.; Dai, H.; Lippard, S. J. Soluble Single-Walled Carbon Nanotubes as Longboat Delivery Systems for Platinum(IV) Anticancer Drug Design. *J. Am. Chem. Soc.* **2007**, *129*, 8438–8439.
19. Dhar, S.; Liu, Z.; Thomale, J.; Dai, H. J.; Lippard, S. J. Targeted Single-Wall Carbon Nanotube-Mediated Pt(IV) Prodrug Delivery Using Folate as a Homing Device. *J. Am. Chem. Soc.* **2008**, *130*, 11467–11476.
20. Graf, N.; Mokhtari, T. E.; Papayannopoulos, I. A.; Lippard, S. J. Platinum(IV)−Chlorotoxin (CTX) Conjugates for Targeting Cancer Cells. *J. Inorg. Biochem.* **2012**, *110*, 58–63.
21. Mukhopadhyay, S.; Barnés, C. M.; Haskel, A.; Short, S. M.; Barnes, K. R.; Lippard, S. J. Conjugated Platinum(IV)−Peptide Complexes for Targeting Angiogenic Tumor Vasculature. *Bioconjugate Chem.* **2008**, *19*, 39–49.
22. Dhar, S.; Gu, F. X.; Langer, R.; Farokhzad, O. C.; Lippard, S. J. Targeted Delivery of Cisplatin to Prostate Cancer Cells by Aptamer Functionalized Pt(IV) Prodrug-PLGA-PEG Nanoparticles. *Proc. Natl. Acad. Sci. U.S.A.* **2008**, *105*, 17356–17361.
23. Kolishetti, N.; Dhar, S.; Valencia, P. M.; Lin, L. Q.; Karnik, R.; Lippard, S. J.; Langer, R.; Farokhzad, O. C. Engineering of Self-Assembled Nanoparticle Platform for Precisely Controlled Combination Drug Therapy. *Proc. Natl. Acad. Sci. U.S.A.* **2010**, *107*, 17939–17944.
24. Dhar, S.; Kolishetti, N.; Lippard, S. J.; Farokhzad, O. C. Targeted Delivery of a Cisplatin Prodrug for Safer and More Effective Prostate Cancer Therapy *in Vivo*. *Proc. Natl. Acad. Sci. U.S.A.* **2011**, *108*, 1850–1855.
25. Graf, N.; Bielenberg, D. R.; Kolishetti, N.; Muus, C.; Banyard, J.; Farokhzad, O. C.; Lippard, S. J. $\alpha_v\beta_3$-Integrin-Targeted PLGA-PEG Nanoparticles for Enhanced Anti-tumor Efficacy of a Pt(IV) Prodrug. *ACS Nano* **2012**, *6*, 4530–4539.
26. Stivaktakis, N.; Nikou, K.; Panagi, Z.; Beletsi, A.; Leondiadis, L.; Avgoustakis, K. PLA and PLGA Microspheres of β-Galactosidase: Effect of Formulation Factors on Protein Antigenicity and Immunogenicity. *J. Biomed. Mater. Res. A* **2004**, *70A*, 139–148.
27. Sirohi, B.; Arnedos, M.; Popat, S.; Ashley, S.; Nerurkar, A.; Walsh, G.; Johnston, S.; Smith, I. E. Platinum-Based Chemotherapy in Triple-Negative Breast Cancer. *Ann. Oncol.* **2008**, *19*, 1847–1852.
28. Staudacher, L.; Cottu, P. H.; Diéras, V.; Vincent-Salomon, A.; Guilhaume, M. N.; Escalup, L.; Dorval, T.; Beuzeboc, P.; Mignot, L.; Pierga, J. Y. Platinum-Based Chemotherapy in Metastatic Triple-Negative Breast Cancer: The Institut Curie Experience. *Ann. Oncol.* **2011**, *22*, 848–856.
29. Giandomenico, C. M.; Abrams, M. J.; Murrer, B. A.; Vollano, J. F.; Rheinheimer, M. I.; Wyer, S. B.; Bossard, G. E.; Higgins, J. D., III. Carboxylation of Kinetically Inert Platinum(IV) Hydroxy Complexes—An Entrée into Orally-Active Platinum(IV) Antitumor Agents. *Inorg. Chem.* **1995**, *34*, 1015–1021.
30. Cohen, S.; Yoshioka, T.; Lucarelli, M.; Hwang, L. H.; Langer, R. Controlled Delivery Systems for Proteins Based on Poly(lactic/glycolic acid) Microspheres. *Pharm. Res.* **1991**, *8*, 713–720.
31. Maeda, H.; Wu, J.; Sawa, T.; Matsumura, Y.; Hori, K. Tumor Vascular Permeability and the EPR Effect in Macromolecular Therapeutics: A Review. *J. Controlled Release* **2000**, *65*, 271–284.
32. Foulkes, W. D.; Smith, I. E.; Reis-Filho, J. S. Triple-Negative Breast Cancer. *N. Engl. J. Med.* **2010**, *363*, 1938–1948.
33. Hayes, D. M.; Cvitkovic, E.; Golbey, R. B.; Scheiner, E.; Helson, L.; Krakoff, I. H. High Dose Cis-platinum Diammine Dichloride: Amelioration of Renal Toxicity by Mannitol Diuresis. *Cancer* **1977**, *39*, 1372–1381.
34. Miller, R. P.; Tadagavadi, R. K.; Ramesh, G.; Reeves, W. B. Mechanisms of Cisplatin Nephrotoxicity. *Toxins* **2010**, *2*, 2490–2518.
35. King, P. D.; Perry, M. C. Hepatotoxicity of Chemotherapy. *Oncologist* **2001**, *6*, 162–176.
36. Yokoyama, M. Drug Targeting with Nano-Sized Carrier Systems. *J. Artif. Organs* **2005**, *8*, 77–84.
37. Hall, M. D.; Hambley, T. W. Platinum(IV) Antitumour Compounds: Their Bioinorganic Chemistry. *Coord. Chem. Rev.* **2002**, *232*, 49–67.
38. Gibbons, G. R.; Wyrick, S.; Chaney, S. G. Rapid Reduction of Tetrachloro(D,L-trans)1,2-diaminocyclohexaneplatinum(IV) (Tetraplatin) in RPMI 1640 Tissue-Culture Medium. *Cancer Res.* **1989**, *49*, 1402–1407.
39. Chaney, S. G.; Wyrick, S.; Till, G. K. In Vitro Biotransformations of Tetrachloro(D,L-trans)-1,2-diaminocyclohexaneplatinum(IV) (Tetraplatin) in Rat Plasma. *Cancer Res.* **1990**, *50*, 4539–4545.
40. Carr, J. L.; Tingle, M. D.; McKeage, M. J. Rapid Biotransformation of Satraplatin by Human Red Blood Cells *in Vitro*. *Cancer Chemother. Pharmacol.* **2002**, *50*, 9–15.

41. Carr, J. L.; Tingle, M. D.; McKeage, M. J. Satraplatin Activation by Haemoglobin, Cytochrome *c* and Liver Microsomes *in Vitro*. *Cancer Chemother. Pharmacol.* **2006**, *57*, 483–490.
42. Bell, D. N.; Liu, J. J.; Tingle, M. D.; Rattel, B.; Meyer, T. U.; McKeage, M. J. Comparative Protein Binding, Stability and Degradation of Satraplatin, JM118 and Cisplatin in Human Plasma *in Vitro*. *Clin. Exp. Pharmacol. Physiol.* **2008**, *35*, 1440–1446.
43. Wexselblatt, E.; Yavin, E.; Gibson, D. Pt(IV) Pro-Drugs with Haloacetato Ligands in the Axial Positions Can Undergo Hydrolysis under Biologically Relevant Conditions. *Angew. Chem., Int. Ed.* **2013**, DOI: 10.1002/anie.201300640.
44. Farokhzad, O. C.; Cheng, J.; Teply, B. A.; Sherifi, I.; Jon, S.; Kantoff, P. W.; Richie, J. P.; Langer, R. Targeted Nanoparticle-Aptamer Bioconjugates for Cancer Chemotherapy *in Vivo*. *Proc. Natl. Acad. Sci. U.S.A.* **2006**, *103*, 6315–6320.
45. Hadeishi, T.; McLaughlin, R. D. Hyperfine Zeeman Effect Atomic Absorption Spectrometer for Mercury. *Science* **1971**, *174*, 404–407.
46. Fernandez, F. J.; Myers, S. A.; Slavin, W. Background Correction in Atomic Absorption Utilizing the Zeeman Effect. *Anal. Chem.* **1980**, *52*, 741–746.
47. Hall, M. D.; Dillon, C. T.; Zhang, M.; Beale, P.; Cai, Z.; Lai, B.; Stampfl, A. P. J.; Hambley, T. W. The Cellular Distribution and Oxidation State of Platinum(II) and Platinum(IV) Antitumour Complexes in Cancer Cells. *J. Biol. Inorg. Chem.* **2003**, *8*, 726–732.
48. McGahan, M. C.; Tyczkowska, K. The Determination of Platinum in Biological Materials by Electrothermal Atomic Absorption Spectroscopy. *Spectrochim. Acta, Part B* **1987**, *42*, 665–668.
49. Probst, R. J.; Lim, J. M.; Bird, D. N.; Pole, G. L.; Sato, A. K.; Claybaugh, J. R. Gender Differences in the Blood Volume of Conscious Sprague–Dawley Rats. *J. Am. Assoc. Lab. Anim. Sci.* **2006**, *45*, 49–52.